# A Study on π/4-DQPSK with Nonredundant Multiple Error Correction

**Seog-Il Song**[a] **and Young-Yearl Han**

**In this paper, to enhance the performance of π/4-DQPSK (π/4-differential quadrature phase shift keying), the scheme using nonredundant multiple error correction is proposed and investigated. This scheme for the differential detection of π/4-DQPSK uses the signal output which is delayed for more than two time slots as the parity check bit and applies it to nonredundant multiple error correction. The proposed system was used for studying the performance of π/4-DQPSK with Nonredundant Error Correction (NEC) in additive white Gaussian noise (AWGN) and Nakagami fade modeled mobile communication channel, and it was observed that the performance increased as the error correction capability increased.**

Manuscript received August 29, 1998; revised April 3, 1999.
[a]Electronic mail: sisong@etri.re.kr

## I. INTRODUCTION

One of the most serious problems that occur in mobile communication systems is the fading of signal amplitude due to multipath channel. Currently, the most accurate model for wireless multipath channel is known as the Nakagami Fading Channel model [1].

To combat the effect of the fading, there are several transmission strategies which could be divided into four basic categories: (1) Those that send a pilot tone with data signal to allow coherent demodulation to be used, such as transparent tone-in-band and tone calibration technique; (2) Those that insert a digital pilot symbol sequence into data stream to measure and compensate for the channel's fading; (3) Those that employ coding which introduce time diversity technique; and (4) Those that employ noncoherent detection to minimize sensitivity of the fading, such as a differential demodulation. In the first three categories, an additional channel bandwidth is required, and the systems are somewhat complex. In comparison with three methods, the noncoherent detection is regarded as a simple method to effectively recover data from faded channels [2]–[6], [24].

π/4-QPSK is an attractive modulation scheme for digital communications because it has a compact spectrum having a reduced envelope fluctuation (compared with conventional QPSK) [7]–[9] and it is easy to demodulate it with non-coherent detection. Its reduced envelope fluctuation introduces less spectral spreading over the nonlinear but power efficient channels.

However, noncoherent detection schemes such as differential detection and discriminator detection suffers from degraded performance when compared with the corresponding coherent detection.

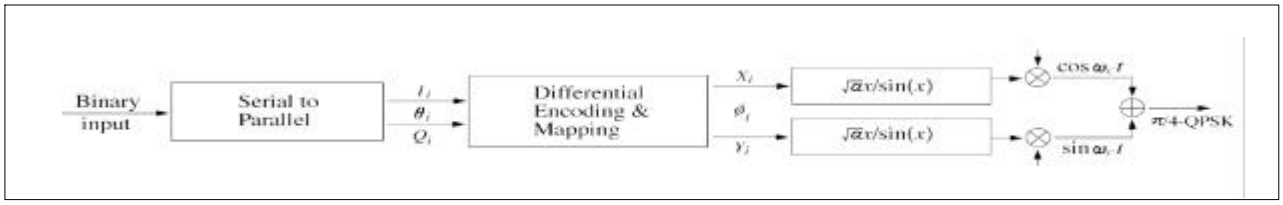


**Fig. 1.** Block diagram of π/4-QPSK modulation.

A particularly attractive method to improve noncoherent detector's performance is the nonredundant error correction (NEC) scheme which does not require any signaling redundancy, any additional bandwidth and additional transmit power. By now, nonredundant single error correction (NSEC) technique has been applied to binary DPSK, multidifferential PSK, DMSK, M-phase DMSK, Duobinary MSK, and π/4-DQPSK [10]–[15].

In this paper, the new type of nonredundant multiple error correction (NMEC) scheme that can correct consecutive errors is applied to π/4-QPSK system. We investigate the performance of π/4-QPSK system with NMEC in the communication channel modeled with Nakagami fading and additive white Gaussian noise. In Section II, π/4-QPSK signaling is briefly reviewed and nonredundant single, double and triple error correction schemes are discussed for π/4-QPSK system. In Section III, the bit error rate (BER) performance of π/4-QPSK system with NMEC is analyzed by computer simulation using acception-rejection method in the communication channel modeled with Nakagami fading and additive white Gaussian noise. Finally, conclusion is given in Section IV.

## II. π/4-QPSK NONREDUNDANT MULTIPLE ERROR CORRECTION

### 1. π/4-QPSK signalling in the transmitter

The block diagram of π/4-QPSK modulation is shown in Fig. 1 where the input signal is split into $I$ channel and $Q$ channel by the serial of parallel converter. $\sqrt{a}$ represents a square root of raised cosine filter with a roll-off factor of α and a Nyquist bandwidth of $f_s/2$ where $f_s$ is the symbol rate. The differential encoder and signal mapper convert $I/Q$ into $X/Y$ using mapping rules of (1).

$$X_i = I_i \cdot X_{i-1} - Q_i \cdot Y_{i-1}$$
$$Y_i = Q_i \cdot X_{i-1} + I_i \cdot Y_{i-1} \quad (1)$$

where the subscripts of $I_i$, $Q_i$, $X_i$ and $Y_i$ represent the timing instances. $I_i$ and $Q_i$ are binary symbols of $\{\mp 0.707\}$ and $X_i$ and $Y_i$ have 5 levels of $\{0, \mp 0.707, \mp 1\}$. The signal mapper can be considered as a converter that transforms the input phase $\theta_i$ to an output phase $\phi_i$ as (2).

$$\phi_i = \phi_{i-1} + \theta_i \quad (2)$$

where $\theta_i = \tan^{-1} Q_i/I_i$, $\phi_i = \tan^{-1} X_i/Y_i$ .

The phase difference between adjacent symbols of π/4-QPSK signal, $\theta_i = \phi_i - \phi_{i-1}$, represents the incoming data $I_i$, $Q_i$. As $\theta_i$ is $\mp\pi/4$ and $\mp 3\pi/4$, the phase $\phi_i$ of π/4-QPSK signal has one of the 8 phase states such as 0, $\mp\pi/4$, $\mp\pi/2$, $\mp 3\pi/4$, and $\pi$. Since the π/4-QPSK signal without phase transition of $\pi$ has less envelope fluctuation compared with conventional QPSK, the π/4-QPSK signal experiences less spectrum spreading over a nonlinear channel [10], [16].

The phase of the modulated output signal at the $i^{th}$ timing instance is written as $\phi_i$ and has one of the eight phase states of 0, $\mp\pi/4$, $\mp\pi/2$, $\mp 3\pi/4$ and $\pi$. From (2), the following results can be obtained

$$\phi_i = \sum_{j=0}^{i} \theta_j, \ \theta_j \in (\pi/4, 3\pi/4, 5\pi/4, 7\pi/4) \quad (3)$$

$$\phi_i - \phi_{i-k} = \sum_{j=0}^{k-1} \theta_{i-j} = \pi/4 \cdot \sum_{j=0}^{k-1} a_{i-j}, a_j \in (1, 3, 5, 7) \quad . \quad (4)$$

Applying Modulo operator to both sides of (4), it is written as follows:

$$\left( \sum_{j=0}^{k-1} a_{i-j} \right)_{\bmod 8} = 4/\pi \cdot (\phi_i - \phi_{i-k})_{\bmod 2\pi} \quad . \quad (5)$$

Using (5), the phase difference $ph_k$ between $i^{th}$ symbol and the symbol delayed by $k$ time slots is shown as (6).

$$ph_1 = (\phi_i - \phi_{i-1})_{\bmod 2\pi} = \pi/4 \cdot (a_i)_{\bmod 8}$$
$$ph_2 = (\phi_i - \phi_{i-2})_{\bmod 2\pi} = \pi/4 \cdot (a_i + a_{i-1})_{\bmod 8}$$
$$ph_3 = (\phi_i - \phi_{i-3})_{\bmod 2\pi} = \pi/4 \cdot (a_i + a_{i-1} + a_{i-2})_{\bmod 8}$$
$$\cdots$$

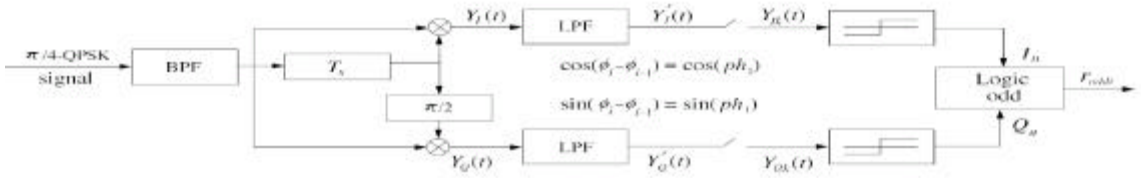


**Fig. 2.** Block diagram of *Ts* differential detection.

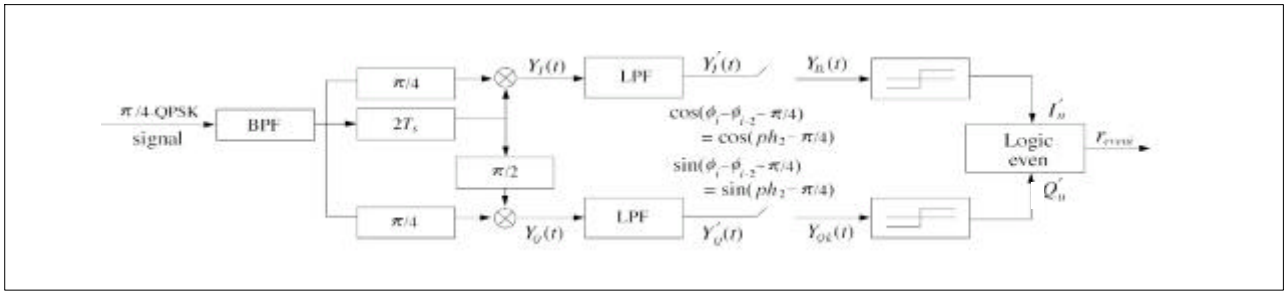


**Fig. 3.** Block diagram of 2*Ts* differential detection.

$$ph_k = (\phi_i - \phi_{i-2})_{\bmod 2\pi} = \pi/4 \cdot (a_i + a_{i-1} \cdots a_{i-k+1})_{\bmod 8} \quad (6)$$

To eliminate $\pi/4$ in (6), we multiply $4/\pi$ on each side and express it as (7) where $\oplus$ represents $(x+y)_{\bmod 8}$ or $(x-y)_{\bmod 8}$, the mod 8 represents the modulo 8 adder.

$$\begin{aligned} PH_1 &= 4/\pi \cdot ph_1 = (a_i)_{\bmod 8} = a_i \\ PH_2 &= 4/\pi \cdot ph_2 = (a_i + a_{i-1})_{\bmod 8} = a_i \oplus a_{i-1} \\ PH_3 &= 4/\pi \cdot ph_3 = (a_i + a_{i-1} + a_{i-2})_{\bmod 8} = a_i \oplus a_{i-1} \oplus a_{i-2} \\ &\cdots \\ PH_k &= 4/\pi \cdot ph_k = (a_i + a_{i-1} \cdots a_{i-k})_{\bmod 8} \\ &= a_i \oplus a_{i-1} \oplus \cdots \oplus a_{j-k} \end{aligned} \quad (7)$$

## 2. Detection of the Data Differential Phase in π/4-QPSK Receiver

The detection of data for received $\pi/4$-QPSK signal means to extract the phase difference, $\theta_i$, between its adjacent symbols. Fig. 2 shows the differential detector to obtain the phase difference between $\pi/4$-QPSK adjacent symbols. BPF eliminates a noise spread out near the carrier frequency. The BPF output signal is multiplied with adjacent symbol produced by a delay element, the delay time of which is equal to time slot width $T_s$. The BPF output signal is also multiplied with $\pi/2$ phase shifted adjacent symbol. The resulting signals are as follows.

$$\begin{aligned} Y_I(t) &= \cos[\omega_c \cdot t + \phi(t)] \cdot \cos[\omega_c \cdot (t - T_s) + \phi(t - T_s)] \\ &= 1/2\{\cos[\omega_c \cdot T_s + \phi(t) - \phi(t - T_s)] + \\ &\quad \cos[2\omega_c \cdot (t - 1/2T_s) + \phi(t) + \phi(t - T_s)]\} \end{aligned} \quad (8)$$

$$\begin{aligned} Y_I(t) &= \cos[\omega_c \cdot t + \phi(t)] \cdot \cos[\omega_c \cdot (t - T_s) + \phi(t - T_s)] \\ &= 1/2\{\cos[\omega_c \cdot T_s + \phi(t) - \phi(t - T_s)] + \\ &\quad \cos[2\omega_c \cdot (t - 1/2T_s) + \phi(t) + \phi(t - T_s)]\} \end{aligned} \quad (9)$$

If the sampling angle frequency, $\omega_c$, satisfies the condition, $\omega_c t = 2\pi n$ ($n$: integer, $t = kT_s$), the in-phase quadrature components $Y_{Ik}$, $Y_{Qk}$ ($Y_{Ik}$ and $Y_{Qk} \in \pm\{\mp 0.707\}$) can be obtained by eliminating the high frequency term shown in (8) and (9) through LPF. Then, these components are sampled and have one of two discrete levels through a threshold detector. Finally, the phase difference between two adjacent symbols is obtained through Logic circuit (=Logic odd) consisting of P/S (Parallel to Serial converter) and phase mapper. As shown in Table 1, in-phase and quadrature components are mapped to $I_{oddi}$, one of odd integer values such as {1, 3, 5, 7} by phase mapper according to the transmitted differential phase data $a_i$.

$$Y'_I(t) = \cos[\phi(t) - \phi(t - T_s)],$$

$$Y'_Q(t) = \sin[\phi(t) - \phi(t - T_s)] \quad (10)$$

$$Y_{IK} = \cos[\phi_k - \phi_{k-1}] = \cos(ph_1),$$

$$Y_{QK} = \sin[\phi_k - \phi_{k-1}] = \sin(ph_1) \quad (11)$$

In a similar manner, Fig. 3 shows that in-phase and quadrature components are obtained for current symbol and the symbol delayed by its $2T_s$ in Fig. 3. The $\pi/4$ phase shifter is included to easily use a simple threshold detector for odd time slot delays [10]. As shown in Table 1, in-phase and quadrature components are mapped to $\lambda_{eveni}$, one of even integer values such as {0, 2, 4, 6} by Logic circuit (= Logic even) consisting of P/S (Parallel to Serial converter) and phase mapper according to the transmitted differential phase data $a_i$. Using this method, various parities can be generated with the received data obtained by passing the received signal through the parity detection circuit.

**Table 1**. The relationship between *Ii*, *Qi* , θi ,*ai* and *In*, *Qu*, γ*oddi*, γ*eveni*.

| $I_i$ $Q_i$ | $\theta_i$ | $a_i$ |
|---|---|---|
| 1 1 | π/4 | 1 |
| −1 1 | 3π/4 | 3 |
| −1 −1 | 5π/4 | 5(−3) |
| 1 −1 | 7π/4 | 7(−1) |

| $I_n$ $Q_u$ | $r_{oddi}$ |
|---|---|
| 1 1 | 1 |
| 0 1 | 3 |
| 0 0 | 5 |
| 1 0 | 7 |

| $I'_n$ $Q'_u$ | $r_{eveni}$ |
|---|---|
| 1 1 | 2 |
| 0 1 | 4 |
| 0 0 | 6 |
| 1 0 | 0 |

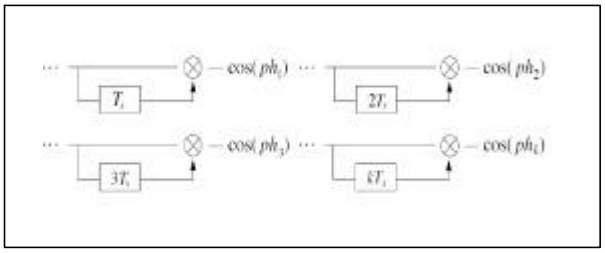


**Fig. 4.** Delay circuits for parity detection.

## 3. Nonredundant Single Error Correction in π/4-DQPSK Receiver

### *A. Parity Generation for Single Error Correction*

To obtain a general method of nonredundant error correction for up to $3\pi/4$-DQPSK signals we use the methods described in [10]−[13]. The following is a description of the nonredundant single error correction for $\pi/4$-DQPSK signal.

Let $\theta_i = \pi/4 \cdot a_i$ and $a_i = \pm 1, \pm 3$ , then the relationship between $a_i$ and data dibit $I_i$, $Q_i$ are given in Table 1. In the receiver, $T_s$ and $2T_s$ delayed differential phase detectors are used to obtain data and parity in the receiver, respectively. In other words, the output of $T_s$ delayed differential phase detector is defined as the phase difference of received carrier between adjacent symbols. In the same way, the output of $2T_s$ delayed differential phase detector is defined as the phase difference of received carrier between the current symbol and its second previous symbol. Let $\lambda_{1i}$ and $\lambda_{2i}$ represent data and parity differential phases at the *i*th sampling instant, respectively, then

$$\lambda_{1i} = \phi'_i - \phi'_{i-1}$$

$$\lambda_{2i} = \phi'_i - \phi'_{i-2} \quad (12)$$

where $\phi'_i$, $\phi'_{i-1}$ and $\phi'_{i-2}$ represent the received carrier phase at $i^{th}$, $(i-1)^{th}$ and $(i-2)^{th}$ sampling instant. Assuming a Nyquist channel without fading and noisefree,

$$\phi'_i = \phi_i, \phi'_{i-1} = \phi_{i-1}, \phi'_{i-2} = \phi_{i-2}, \quad \text{hence}$$

$$\lambda_{1i} = \theta_i = \pi/4 \cdot a_i \quad (13)$$

$$\lambda_{2i} = (\theta_i + \theta_{i-1}) \bmod 2\pi = \pi/4 (a_i + a_{i-1}) \bmod 8 \quad (14)$$

By eliminating $\pi/4$ at the above equations, normalized data and parity differential phases can be obtained in (15).

$$\lambda_{1i} = a_i \in (1, 3, 5, 7)$$

$$\lambda_{2i} = (a_i + a_{i-1}) \bmod 8 \in (0, 2, 4, 6) \quad (15)$$

If there are some errors caused by intersymbol interference and noise, normalized data and parity differential phases are expressed as follows.

$$\lambda_{1i} = (a_i + e_{1i}) \bmod 8 = a_i \oplus e^{d_i} \quad (16)$$

$$\lambda_{2i} = (a_i + a_{i-1} + e_{2i}) \bmod 8 = a_i \oplus a_{i-1} \oplus e^{P_i} \quad (17)$$

where $e_{1i}(=e^{d_i})$ and $e_{2i}(=e^{P_i})$ represent errors included within data and parity differential phases, respectively. The errors $e_{1i}$ and $e_{2i}$ could be 0, $\pm 2$ and $\pm 4$. The data and parity shown in (15) is equivalent to those in the case of 1/2 single error correcting self orthogonal convolutional code [17]. Therefore, for error correction, the parity obtained in the receiver is possibly used without additional encoding in the transmitter.

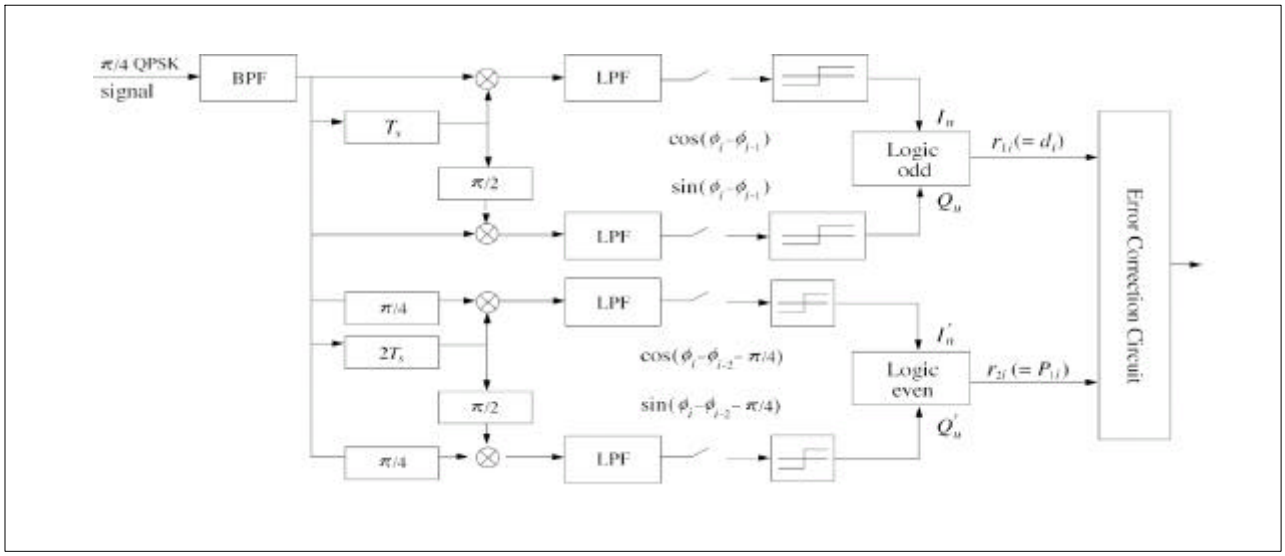


**Fig. 5.** Block diagram of differential detection of π/4-DQPSK with single NEC.

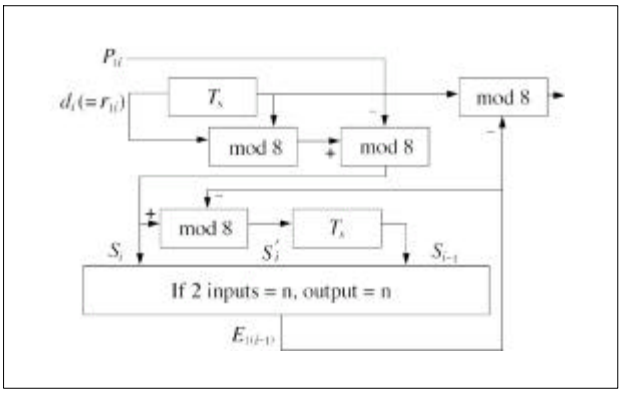


**Fig. 6.** Block diagram of general scheme of NEC for π/4-QPSK.

### *B. Syndrome Generation for Single Error Correction*

Syndrome feedback decoding [12] technique is used to correct errors contained in the data with the data and parity obtained above. The block diagram of the syndrome feedback decoder is shown in Fig 6. We use $\lambda_{1i}$, its one bit delay $\lambda_{1(i-1)}$ and $\lambda_{2i}$ to generate syndromes $S_i$. Equations (18) and (19) can be expressed using $\lambda_{1i}(=d_i)$, $\lambda_{1(i-1)}(=d_{i-1})$ which is a one bit delayed output of $\lambda_{1i}$, and $\lambda_{2i}(=p_{1i})$ which is parity receive detection.

$$\begin{aligned} S_i &= (\lambda_{1i}+\lambda_{1(i-1)}-\lambda_{2i}) \bmod 8 \\ &= a_i \oplus e^{d_i} \oplus a_{i-1} \oplus e^{d_{i-1}} \oplus a_i \oplus a_{i-1} \oplus e^{P_i} \\ &= (e^{d_i}+e^{d_{i-1}}-e^{P_i}) \bmod 8 = e^{d_i} \oplus e^{d_{i-1}} \oplus e^{P_i} \end{aligned} \quad (18)$$

$$S'_i = (S_i - E_{1(i-1)}) \bmod 8 \quad (19)$$

where $E_{1(i-1)}$ is the estimation of the error $e^{d_{i-1}}(=e_{1(i-1)})$. If it is assumed that the error $e^{d_{i-1}}$ is correctly estimated or is zero, (20) is satisfied.

$$S_{i-1} = (S'_{i-1}) \bmod 8 = (e_{1(i-1)} - e_{2(i-1)}) \bmod 8 \quad = e^{d_{i-1}} \oplus e^{P_{i-1}} \quad (20)$$

If there is only one nonzero element among the $e^{d_i}$, $e^{d_{i-1}}$, $e^{P_{i-1}}$, the error $e^{d_{i-1}}$ can be correctly determined. $E_{1(i-1)}$ is zero if $S_i \neq S_{i-1}$, and $n$ ($n \in \{1, 3, 5, 7\}$) if $S_i = S_{i-1} = n$. Therefore, the output data can be correctly recovered by subtracting $E_{1(i-1)}$ from $\lambda_{1(i-1)}$.

## 4. Nonredundant Double Error Correction in π/4-QPSK Receiver

### *A. Parity Generation for Double Error Correction*

As shown in Fig. 7, the parity for double error correction, $P_{2i}$, is generated using $\lambda_{2(i-1)}$ and $\lambda_{6i}$, where $\lambda_{2(i-1)}$ is the one bit delay of the phase difference of received carriers between the current symbol and its two bit delayed symbol. And $\lambda_{6i}$ is the phase difference of received carriers between the current symbol and its six bit delayed symbol. That is, as shown in (21), the parity $P_{2i}$ is obtained by subtracting $a_{i-1} \oplus a_{i-2}$ (the output of $2T_s$ delayed differential phase detector in Fig. 7) from $a_i \oplus a_{i-1} \oplus a_{i-2} \oplus a_{i-3} \oplus a_{i-4} \oplus a_{i-5}$ (the output of $6T_s$ delayed differential phase detector in Fig. 7). In Fig. 7, the operation rules of the Logic odd and Logic even are shown in Table 1.

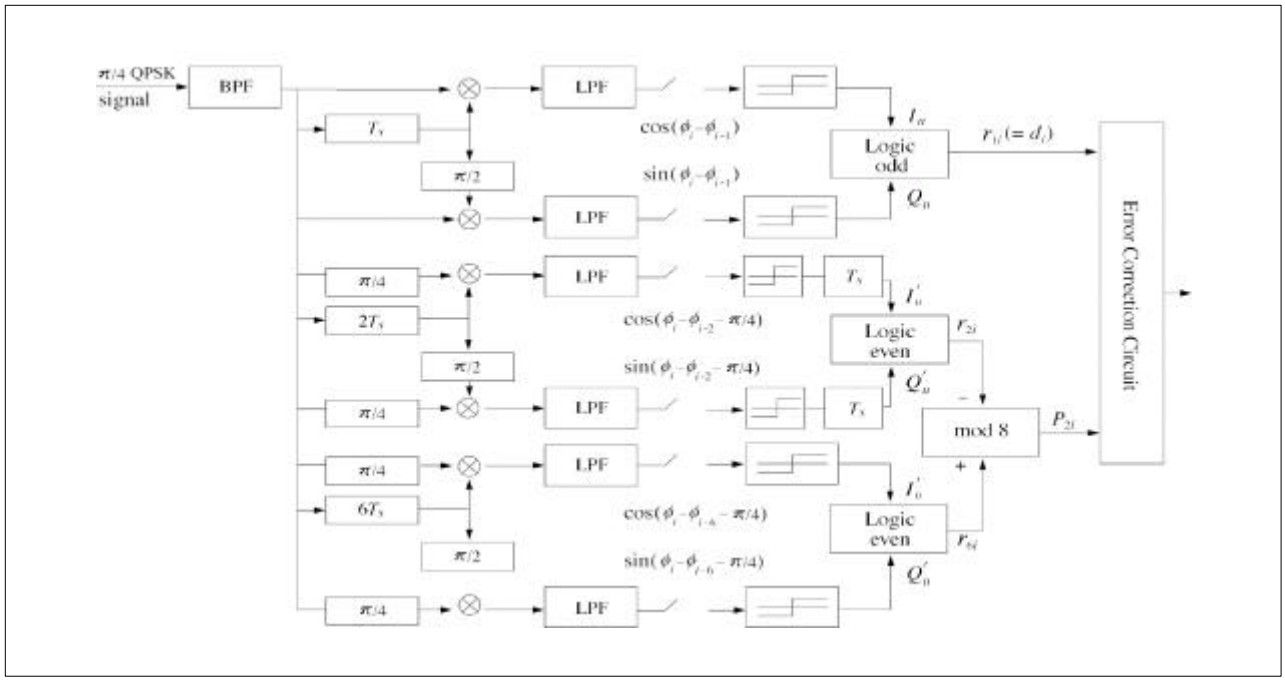


**Fig. 7.** Block diagram of differential detection of π/4-QPSK with double NEC.

$$P_{2i} = a_i \oplus a_{i-3} \oplus a_{i-4} \oplus a_{i-5} \tag{21}$$

*B. Syndrome Generation for Double Error Correction*

Equation (21) corresponds to 1/2 double error correcting orthogonal convolutional code [18]. Hence, syndromes are formed as follows:

$$\begin{aligned}
S_{i-5} &= e^{P_{i-5}} \oplus e^{d_{i-5}} \\
S_{i-4} &= e^{P_{i-4}} \oplus e^{d_{i-4}} \\
S_{i-3} &= e^{P_{i-3}} \oplus e^{d_{i-3}} \\
S_{i-2} &= e^{P_{i-2}} \oplus e^{d_{i-2}} \oplus e^{d_{i-5}} \\
S_{i-1} &= e^{P_{i-1}} \oplus e^{d_{i-1}} \oplus e^{d_{i-4}} \oplus e^{d_{i-5}} \\
S_i &= e^{P_i} \oplus e^{d_i} \oplus e^{d_{i-3}} \oplus e^{d_{i-4}} \oplus e^{d_{i-5}}
\end{aligned} \tag{22}$$

where $e^{d_i}$, $e^{P_i}$ are errors of the data and the parity at the $i^{th}$ sampling instant, respectively. Figure 8 shows how syndromes described as the above equation are generated.

Syndrome feedback decoder for double error correction is Implemented using four regenerated syndromes shown in (23).

$$\begin{aligned}
S_{i-5} &= e^{P_{i-5}} \oplus e^{d_{i-5}} \\
S_{i-2} &= e^{P_{i-2}} \oplus e^{d_{i-2}} \oplus e^{d_{i-5}}
\end{aligned}$$

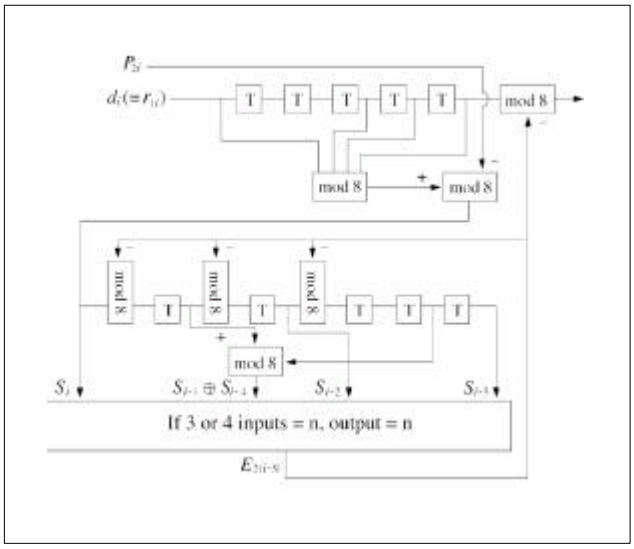


**Fig. 8.** Block diagram of general scheme of double NEC for π/4-QPSK.

$$\begin{aligned}
S_{i-4} \oplus S_{i-1} &= e^{P_{i-1}} \oplus e^{d_{i-1}} \oplus e^{P_{i-4}} \oplus e^{d_{i-5}} \\
S_i &= e^{P_i} \oplus e^{d_i} \oplus e^{d_{i-3}} \oplus e^{d_{i-4}} \oplus e^{d_{i-5}}
\end{aligned} \tag{23}$$

Here, we know that all of syndromes shown in (23) commonly include the error term, $e^{d_{i-5}}$ but data error terms of $e^{d_i}$, $e^{d_{i-1}}$,, $e^{d_{i-2}}$ and $e^{d_{i-4}}$ do not appear repetitively in four syndromes, where such set of equation is said to be orthogonal on $e^{d_{i-5}}$.

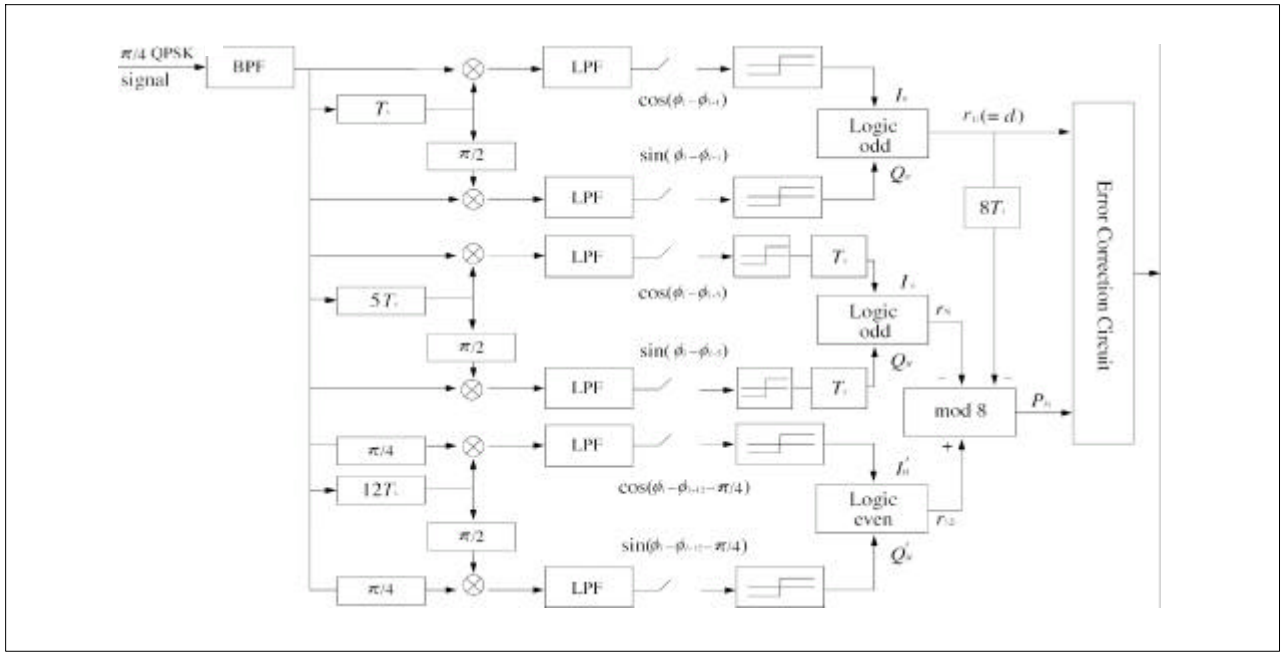


**Fig. 9.** Block diagram of differential detection of π/4-QPSK with triple NEC.

As shown in Fig. 8, the process to correct the error of the five bit delayed data, $\lambda_{1(i-5)}$ is described as follows: In syndrome feedback decoder, the estimated error, $e^{d_{i-5}}$ of $\lambda_{1(i-5)}$ returns back to obtain four regenerated syndromes. The estimated error can be determined by applying the rule of maximum likelihood to four regenerated syndromes. Finally, the data can be corrected by subtracting the estimated error from the contaminated original data.

How to get the estimation of the error using the rule of maximum likelihood between four regenerated syndromes is explained in more detail as follows: If $e^{d_{i-5}}$ has the value of $n$ ($n \in \{1, 3, 5, 7\}$) and no other errors exist, all syndromes are equal to $n$. If $e^{d_{i-5}}$ has the value of $n$ and another error variable in the 12 error variables has the same value as $n$, then three of four regenerated syndromes are equal to $n$ and the other syndrome becomes zero. From these cases, it is evident that the error $e^{d_{i-5}}$ has the value of $n$ if more than three of regenerated syndromes have the same value as $n$. On the other hand, if only one error other than $e^{d_{i-5}}$ has the value of $n$ and the rest of errors do not exist, then the only syndrome containing this error becomes $n$ and the rest of other syndromes become zero. If two errors other than $e^{d_{i-5}}$ have the value of $n$, then two syndromes become $n$ in most cases. From the above two cases, we can say that if errors other than $e^{d_{i-5}}$ occurs, at most two syndromes have the same value. In conclusion, while at most two errors occur, the estimated error, $E_{2(i-5)}$ of $\lambda_{1(i-5)}$ can be determined to have the value of $n$ if more than three of syndromes have the same value as $n$.

Finally, the five bit delay, $\lambda_{1(i-5)}$ of the data input $\lambda_{1i}$ is corrected by subtracting the estimated error, $E2(i-5)$ from the contaminated data, $\lambda_{1(i-5)}$.

## 5. Nonredundant Triple Error Correction in π/4-DQPSK Receiver

In a similar manner as the double error correction, the triple error correction can be achieved and is described in this subsection.

### *A. Parity Generation for Triple Error Correction*

As shown in Fig. 9, the parity differential phase for triple error correction, $P_{3i}$ is generated using $\lambda_{1(i-8)}$, $\lambda_{5(i-1)}$ and $\lambda_{12i}$, where $\lambda_{1(i-8)}$ is the eight bit delay of the data, $\lambda_{5(i-1)}$ is the one bit delay of the phase difference of received carriers between the current symbol and its five bit delayed symbol and $\lambda_{12i}$ is the phase difference of received carriers between the current symbol and its twelve bit delayed symbol, respectively. That is, as shown in (26), the parity $P_{3i}$ is obtained by subtracting $a_{i-1} \oplus a_{i-2} \oplus a_{i-3} \oplus a_{i-4} \quad \oplus a_{i-5}$ (the output of $5T_s$ delayed differential phase detector in Fig. 9) and $a_{i-8}$ (the

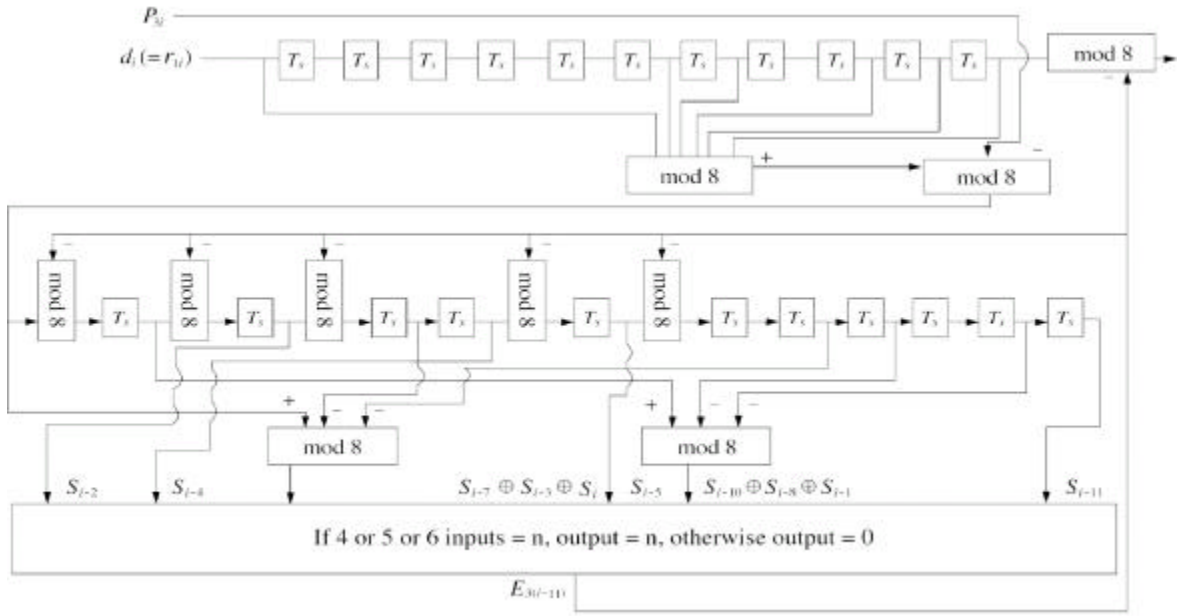


**Fig. 10.** Block diagram of general scheme of triple NEC for $\pi/4$-DQPSK.

$8T_s$ delay of $T_s$ delayed differential phase detector in Fig. 9) from $a_i \oplus a_{i-1} \oplus a_{i-2} \oplus \cdots \oplus a_{i-10} \oplus a_{i-11}$ (the output of $12T_s$ delayed differential phase detector in Fig. 9). In Fig. 9, the operation rules of the Logic odd and Logic even are shown in Table 1.

$$P_{3i} = a_i \oplus a_{i-6} \oplus a_{i-7} \oplus a_{i-9} \oplus a_{i-10} \oplus a_{i-11} \tag{24}$$

### *B. Syndrome Generation for Triple Error Correction*

Equation (24) corresponds to 1/2 triple error correcting orthogonal convolutional code [17]. Hence, syndromes are formed as follows:

$$S_{i-11} = e^{P_{i-11}} \oplus e^{d_{i-11}}$$

$$S_{i-10} = e^{P_{i-10}} \oplus e^{d_{i-10}}$$

$$S_{i-9} = e^{P_{i-9}} \oplus e^{d_{i-9}}$$

$$S_{i-8} = e^{P_{i-8}} \oplus e^{d_{i-8}}$$

$$S_{i-7} = e^{P_{i-7}} \oplus e^{d_{i-7}}$$

$$S_{i-6} = e^{P_{i-6}} \oplus e^{d_{i-6}}$$

$$S_{i-5} = e^{P_{i-5}} \oplus e^{d_{i-11}} \oplus e^{d_{i-5}}$$

$$S_{i-4} = e^{P_{i-4}} \oplus e^{d_{i-11}} \oplus e^{d_{i-10}} \oplus e^{d_{i-4}}$$

$$S_{i-3} = e^{P_{i-3}} \oplus e^{d_{i-10}} \oplus e^{d_{i-9}} \oplus e^{d_{i-3}}$$

$$S_{i-2} = e^{P_{i-2}} \oplus e^{d_{i-11}} \oplus e^{d_{i-9}} \oplus e^{d_{i-8}} \oplus e^{d_{i-2}}$$

$$S_{i-1} = e^{P_{i-1}} \oplus e^{d_{i-11}} \oplus e^{d_{i-10}} \oplus e^{d_{i-8}} \oplus e^{d_{i-7}} \oplus e^{d_{i-1}}$$

$$S_i = e^{P_i} \oplus e^{d_{i-11}} \oplus e^{d_{i-10}} \oplus e^{d_{i-9}} \oplus e^{d_{i-7}} \oplus e^{d_{i-6}} \oplus e^{d_i} \tag{25}$$

where $e^{d_i}$, $e^{P_i}$ are errors of the data and the parity at the $i^{th}$ sampling instant, respectively. Fig. 10 shows how syndromes described as the above equation are generated.

Syndrome feedback decoder for triple error correction is implemented using six regenerated syndromes shown in (26).

$$S_{i-11} = e^{P_{i-11}} \oplus e^{d_{i-11}}$$

$$S_{i-5} = e^{P_{i-5}} \oplus e^{d_{i-5}} e^{d_{i-11}}$$

$$S_{i-4} = e^{P_{i-4}} \oplus e^{d_{i-4}} e^{d_{i-10}} e^{d_{i-11}}$$

$$S_{i-2} = e^{P_{i-2}} \oplus e^{d_{i-2}} e^{d_{i-8}} e^{d_{i-9}} e^{d_{i-11}}$$

$$S_{i-10} \oplus S_{i-8} \oplus S_{i-1} = e^{P_{i-1}} \oplus e^{d_{i-1}} \oplus e^{P_{i-4}} \oplus e^{d_{i-5}} \oplus e^{d_{i-11}}$$

$$S_{i-7} \oplus S_{i-3} \oplus S_i = e^{P_i} \oplus e^{P_{i-3}} \oplus e^{P_{i-7}} \oplus e^{d_i} \oplus e^{d_{i-3}} \oplus e^{d_{i-6}} \oplus e^{d_{i-11}} \tag{26}$$

Here, as in the case of double error correction, all of the regenerated syndromes shown in (26) commonly include the error term, $e^{d_{i-11}}$ and data error terms except $e^{d_{i-11}}$ do not

appear repetitively in six regenerated syndromes, where such set of equation is said to be orthogonal on $e^{d_{i-11}}$. Like the syndrome equations related with $e^{d_{i-5}}$ and the other 12 error variables in (23), the received error can be corrected if there are less than three errors in the error variables which do not contain zero in the relationship between $e^{d_{i-11}}$ and other error variables. It is evident that the error $e^{d_{i-11}}$ decided by the majority logic has the value of $n$ if more than four of the regenerated syndromes in (26) have the same value as $n$.

In conclusion, while at most three errors occur, the estimated error, $E_{3(i-11)}$ of $\lambda_{1(i-11)}$ can be determined to have the value of $n$ if more than four of syndromes have the same value as $n$. Finally, the eleven bit delay, $\lambda_{1(i-11)}$ of the data input $\lambda_{1i}$ is corrected by subtracting the estimated error, $E_{3(i-11)}$ from the contaminated data, $\lambda_{1(i-11)}$.

**Fig. 11.** Example of error correction of nonredundant error correction (NEC) for $\pi/4$-DQPSK.

Figures 11(b) and 11(c) explain examples of three nonredundant multiple error correction schemes of $\pi/4$-DQPSK data. In Fig. 11, $a_i$ is the transmitted original data, $\lambda_{1i}$ $(= d_i)$'s are received data for three error correction schemes, and the dotted box indicates error occurrence. $P_{1i}$, $P_{2i}$ and $P_{3i}$ are generated parities for three error correction schemes, where we assume that the generated parity has no error. In single error correction scheme of Fig. 11(a), it is possible to correct received data perfectly when only one error occurs without any adjacent error. However, it cannot correct the received data when two consecutive errors occur. In double error correction scheme of Fig. 11(b), it is noticeable that correction is made for the two consecutive errors that occur in delayed sections where parity is generated, but can not correct more than two errors. In Fig. 11(c), three consecutive errors are corrected accurately in delayed sections where parity is generated.

## III. $\pi/4$-DQPSK NEC Computer Simulation

The probability density function (pdf) of the phase error due to Gaussian noise in the coherent detector is written in (27) [19].

$$f(\theta) = e^{-R}/2\pi + \frac{1}{2}\sqrt{\frac{R}{\pi}}\exp(-R\sin^2\theta) \cdot \cos\theta(1+erf(\sqrt{R}\cos\theta)), \quad (27)$$

where $-\pi \le \theta \le \pi$, $\theta$ : phase error,
$R$ : Signal to Noise Ratio (S/N)

The pdf of the phase error due to Nakagami fading in coherent detection can be derived as follows. In the general BPSK coherent demodulator, the received signal $S(t)$ is mixed with an additive noise $n_b(t)$.

$$S(t) = d\cos\omega_c t + n_b(t) \quad (28)$$

From $n_b(t) = n_c\cos\omega_c t - n_s\sin\omega_c t$, the signal is split into in-phase component $x = d + n_c = A\cos\theta$, quadrature component $y = n_s = A\sin\theta$, where $A = \sqrt{x^2 + y^2}$, $\theta = \tan^{-1} y/x$. The statistical characteristics of the in-phase and quadrature components of a noise i.e., $n_c$ and $n_s$, have the same Gaussian distribution with zero mean and standard deviation $\sigma$, respectively. And these two random variables are statistically independent of each other. The pdf of the signal amplitude $d$ influenced by Nakagami fading, is expressed as follows [20].

$$f_D(d) = \frac{2m^m d^{2m-1}}{\Gamma(m)\Omega^m} e^{\frac{-md^2}{\Omega}}, \quad (29)$$

where $d > 0$, $m \geq 1/2$, $\Omega = E[d^2]$,
$\Gamma(\cdot)$ : Gamma function,
$m$ : Nakagami fading factor

By obtaining the joint pdf of $x$ and $y$ at first and transforming it to the pdf of $A$ and $\theta$, the pdf of the phase error due to Nakagami fading can be solved [21]. Since $d$ and $n_c$ are independent of each other, the pdf of $x$, $f(x)$ can be obtained as (30).

$$f(x) = \int_{-\infty}^{\infty} f_{D,N_c}(d, x-d)\, d\,\mathrm{d}$$

$$= \frac{2m^m e^{\frac{-x^2}{2\sigma_n^2}}}{\Gamma(m)\sigma^m\sqrt{2\pi\sigma_n^2}} \int_0^{\infty} d^{2m-1} e^{-Kd^2+\left(\frac{x}{\sigma_n^2}\right)d}\, d\,\mathrm{d}, \qquad (30)$$

where $K = \frac{m}{\sigma} + \frac{1}{2\sigma_n^2}$ .

Using the following formula, $f(x)$ is obtained as (32) (See p. 337 in [23]):

$$\int_0^{\infty} x^{(\lambda-1)} e^{-\beta x^2 - \lambda x}\,\mathrm{d}x = (2\beta)^{-\frac{\lambda}{2}}\Gamma(\lambda) e^{\frac{\lambda^2}{8\beta}} D_{-\lambda}\left(\frac{\lambda}{\sqrt{2\beta}}\right), \qquad (31)$$

where $\beta > 0$, $\lambda > 0$

$$f(x) = \frac{m^m\Gamma(2m)}{\sqrt{\pi\sigma_n^2}\sigma^m K^m\Gamma(m)2^{m-\frac{1}{2}}} e^{-\frac{4K\sigma_n^2-1}{8K\sigma_n^4}x^2} \cdot D_{-2m}\left(\frac{-x}{\sqrt{2k\sigma_n^2}}\right), \qquad (32)$$

where $-\infty < x < \infty$, $D_v(x)$ is called as a parabolic cylinder function defined in (33) (See p. 1064 in [23]).

$$D_{\lambda}(x) = \frac{e^{-\frac{x^2}{4}}}{\Gamma(-\lambda)} \int_0^{\infty} e^{-xy-\frac{y^2}{2}} y^{-\lambda-1}\,\mathrm{d}y \qquad (33)$$

where $\lambda < 0$.

Since $x$ and $y$ are independent of each other, the joint pdf of two random variables $x$ and $y$ is obtained by multiplying each pdf.

$$f(x,y) = \frac{m^m\Gamma(2m)e^{-\frac{4K\sigma_n^2(x^2+y^2)-x^2}{8K\sigma_n^4}}}{\pi\sigma_n^2\sigma^m K^m\Gamma(m)2^m} \cdot D_{-2m}\left(\frac{-x}{\sqrt{2K\sigma_n^2}}\right) \qquad (34)$$

From $x = d + n_c = A\cos\theta$ and $y = n_s = A\sin\theta$ , the pdf function of $A$ and $\theta$ is solved by transforming the pdf of $x$ and $y$.

$$f(A,\theta) = \frac{A}{2\pi\Omega^2} e^{-la^2} D_{-2m}(-Ab) \qquad (35)$$

where $\frac{1}{2\sigma^2} = \frac{m^m\Gamma(2m)}{\sigma_n^2(2K\sigma)^m\Gamma(m)}$

$b = \frac{\cos\theta}{\sqrt{2K\sigma_n^2}}$

$l = \frac{4K\sigma_n^2 - \cos^2\theta}{8K\sigma_n^4}$ .

Calculating the integral for amplitude $A$ in (35) results to the pdf of the phase error $\theta$ as follows:

$$f(\theta) = \int_0^{\infty} \frac{A}{2\pi\Omega^2} e^{-la^2} D_{-2m}(-Ab)\,\mathrm{d}A$$

$$= \int_0^{\infty} \frac{A\cdot 2^{-m} e^{-(\frac{l+b^2}{4})A^2}}{2\sqrt{\pi}\Omega^2\Gamma(m+\frac{1}{2})} \cdot {}_1F_1\left(m; \frac{1}{2}; \frac{A^2b^2}{2}\right)\mathrm{d}A$$

$$+ \int_0^{\infty} \frac{A^2b\cdot 2^{-m} e^{-(l+\frac{b^2}{4})A^2}}{\sqrt{2\pi}\Omega^2\Gamma(m)} \cdot {}_1F_1\left(m+\frac{1}{2}; \frac{3}{2}; \frac{A^2b^2}{2}\right)\mathrm{d}A \qquad (36)$$

The pdf of the phase error due to Nakagami fading, by integrating and then placing $K$, $\frac{1}{2\sigma^2}$, $b$, $l$ in (36) is as (37), where the S/N ratio, $R$, is $\frac{\sigma}{2\sigma_n}$ and ${}_1F_1(\cdot)$, ${}_2F_1(\cdot)$, are hyper geometry functions (See p. 1045 in [23]) which are as (38).

$$f(\theta) = \frac{1}{2\pi}\left(\frac{m}{m+R}\right)^m {}_2F_1\left(1, m, \frac{1}{2}, \frac{R\cos^2\theta}{m+R}\right)$$

$$+ \frac{2^{-2m}\Gamma(2m)}{\Gamma^2(m)}\sqrt{\frac{R}{m+R}}\cos\theta\left(\frac{m}{m+R}\right)^m$$

$$\cdot {}_2F_1\left(m+\frac{1}{2}, \frac{3}{2}, \frac{3}{2}, \frac{R\cos^2\theta}{m+R}\right) \qquad (37)$$

where $-\pi \leq \theta \leq \pi$

$${}_1F_1(\alpha;\lambda,z) = \frac{\Gamma(\lambda)}{\Gamma(\alpha)}\sum_{k=0}^{\infty}\frac{\Gamma(\alpha+k)}{\Gamma(\lambda+k)}\frac{z^k}{k!}$$

$${}_2F_1(\alpha;\beta;\lambda,z) = \frac{\Gamma(\lambda)}{\Gamma(\alpha)\Gamma(\beta)}\sum_{k=0}^{\infty}\frac{\Gamma(\alpha+k)\Gamma(\beta+k)}{\Gamma(\lambda+k)}\frac{z^k}{k!} \qquad (38)$$

In coherent detection, errors occur when the phase error is altered to the error domain, whereas in differential detection, they occur when the sum of the phase error in the two successive time intervals is transited to the error

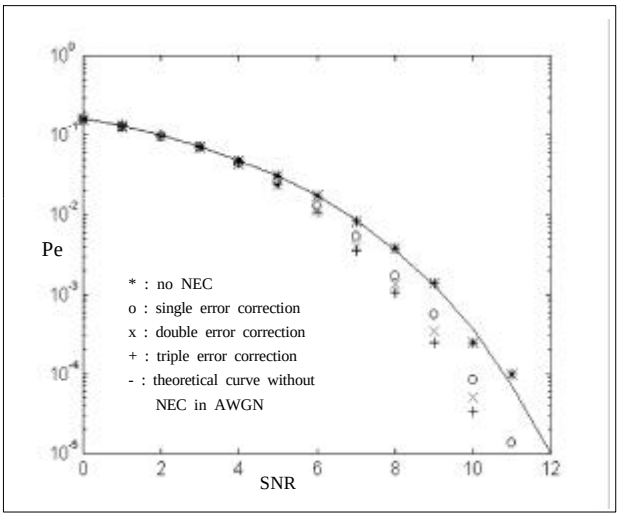


**Fig. 12.** Bit-Error-Rate (BER) performance of $\pi/4$-DQPSK with NEC in AWGN.

domain. Therefore, making the reasonable assumption that the additive noise samples in the two successive time intervals are independent, the probability density of the phase difference can be obtained by convolving the density function of the phase error due to Gaussian noise in the coherent detector with itself [22]; namely,

$$f(\triangle\theta) = \int_{-\pi}^{\pi} f(\theta) f(\triangle\theta + \theta) d\theta \qquad (39)$$

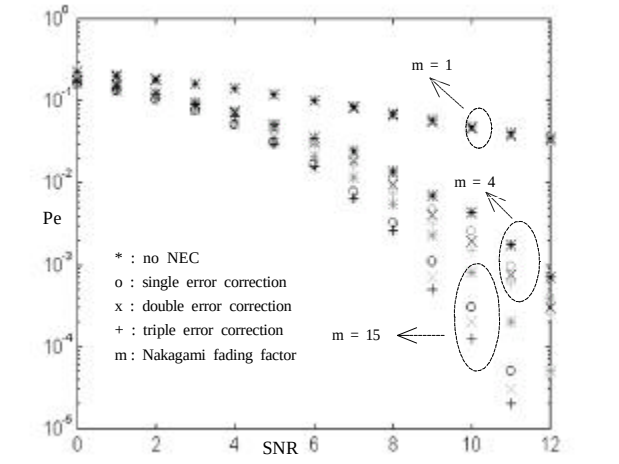


**Fig. 13.** BER performance of $\pi/4$-DQPSK with NEC in Nakgami fading.

where the random variable $\triangle\theta$ is defined in terms of the noise phase component in the two successive time intervals. It is difficult to solve this equation accurately, so it can be considered as a convolution. Acception-Rejection method [13] is used to simulate the performance of $\pi/4$-DQPSK system with nonredundant error correction. Acception-Rejection method is applicable when the probability density function, $f(x)$, has an upper and lower limit of a $x$'s range, and an upper bound of $f(x)$. When the cumulative distribution can not be integrated and inverted, the Acception-Rejection method is a convenient method for generating random numbers of desired probability density function. Data and parity are made by adding generated random phase error that satisfies $f(\theta)$ to the phase that is generated by Pseudo random Number (PN) code.

The data without the error correction circuit and the corrected data with the error correction circuit are compared to investigate the Bit-Error-Rate (BER) performance of $\pi/4$-DQPSK with NEC. The simulation results of BER performance in AWGN environment and in Nakagami fading with AWGN environment, are shown in Fig. 12 and Fig. 13, respectively. It proves out that nonredundant multiple error correction scheme for $\pi/4$-QPSK can improve the performance in both AWGN and Nakagami fading with AWGN environment. The theoretical $\pi/4$-DQPSK demodulation curve [22] is included as a reference for error correction capability. Specially, we can see that our simulation results in AWGN consists to those published in the reference [10]. More improvement is possibly obtained as Nakagami fading factor ($m$) and the number of error correction order increase. An improvement at a BER of $10^{-4}$ in AWGN can be achieved more than 1.2 dB. At $m$=15, we can get improvement more than 1 dB in Nakagami fading with AWGN environment.

## IV. CONCLUSION

In this paper, a method for increasing the performance of $\pi/4$-DQPSK ($\pi/4$-differential quadrature phase shift keying) using nonredundant multiple error correction is proposed and investigated by using the relationship between the present differential demodulation and $k$ order differential detector. This error correction method is based on orthogonal convolutional code error correction which can be demodulated using a simple circuit. The complexity of the error correction design depends on the generation matrix of the orthogonal convolutional code. The performance of the nonredundant multiple error correction was studied using an additive white Gaussian noise and Nakagami fading modeled channel with the method of

Acception-Rejection. The BER curve of Fig. 12 shows that 1.2 dB improvement is achived at a BER of $10^{-4}$ for AWGN environment by a single error correction. It is also seen that the BER performance was improved as the number error correction increased. In Fig. 13, we can also see that more than 1 dB improvement is achived by single error correction at a BER of $10^{-4}$ for Nakagami fading with $m=15$ and AWGN environment, and the performance increased as the Nakagami fading factor, $m$, increased. The computer simulation was held assuming that the error occurs independently on data and parity, but practically, if error occurs to the data, the probability of error occurring to the parity increases. Therefore, the performance will be somewhat lower. Using nonredundant error correction methods by adding a simple circuit to the receiver will make a suitable performance gain without requiring additional bandwidth or transmission power.

## REFERENCES


[1] U. Charsh, "Reception through Nakagami Fading Multipath Channels with Random Delays," *IEEE Trans. Commun.*, Vol. COM−27, Apr. 1979, pp. 657−670.

[2] J. P. McGeehan and A. J. Bateman, "Phase-Locked Transparent Tone-in-Band (TTIB): A New Spectrum Configuration Particularly Suited to the Transmission of Data over SSB Mobile Radio Network," *IEEE Trans. Commun.* Vol. COM−32, Jan. 1984.

[3] F. Davarian, "Mobile Digital Communications Via Tone Calibration," *IEEE Trans. Veh. Tech.*, Vol. VT−36, May 1987, pp. 55−62.

[4] S. Sampei and T. Sunaga, "Rayleigh Fading Compensation Method for 16−QAM in Digital Land Mobile Radio Channel," *Proceedings IEEE Vehicular Technology Conference*, San Francisco, 1989, pp. 640−646.

[5] E. Lutz, "Code and Interleave Design for Data Transmission over Fading Channel," *Proceedings Global Telecommunications Conference*, 1984, pp. 12.4.1−12.4.6.

[6] M. K. Simon and C. C.Wang, "Differential Detection of Gaussian MSK in a Mobile Radio Environment," *IEEE Trans. Veh. Tech.*, Vol. VT−33, Nov. 1984, pp. 307−320.

[7] S. Chennakeshu and G. J. Saulnier, "Differential Detection of pi/4-shifted-DQPSK for Digital Celluar Radio," *IEEE Trans. on Veh. Tech.*, Vol. VT−42, Feb. 1993, pp. 46−57.

[8] P. Varshney and S. Kumar, "Performance of North American Digital Cellular System with Frequency-offset Diversity and Differential Detection," *Proceedings of the IEEE International Communications Conference*, Seattle, Washington, 1995.

[9] C. S. Ng, T. T. Tjhung, F. Adachi, and K.M. Lye, "On the Error Rates of Differentially Detected Narrowband pi/4-DQPSK in Rayleigh Fading and Gaussian Noise," *IEEE Trans. on Veh. Tech.*, Vol. VT−42, Aug. 1993, pp. 259−265.

[10] J. Yang and K. Feher, "An Improved $\pi/4$-QPSK with Nonredundant Error Correction for Satellite Mobile Broadcasting," *IEEE Trans. on Broad.*, Vol. VT−37, March 1991, pp. 9−16.

[11] T. Masamura, S. Samejima, Y. Morihiro, and H. Fuketa, "Differential Detection of MSK with Nonredundant Error Correction," *IEEE Trans. Commun.*, Vol. COM−27, June 1979, pp. 912−918.

[12] S. Samejima, K. Enomoto, and Y. Watanabe, "Differential PSK System with Nonredundant Error Correction," *IEEE J. Selected Areas Commun.*, Vol. SAC−1, Jan. 1983, pp. 74−82.

[13] Y. Han and J. Choi, "DMSK System with Nonredundant Error Correction Capability," *Proceedings of the IEEE GLOBCOM Conference*, San Francisco, 1991, pp. 770−774.

[14] Gary D. Boudreau and Peter J. Mclane, "Defferential Detection of Duobinary CPFSK," *IEEE Trans. Commun.*, Vol. COM−35, Feb. 1987, pp. 181−184.

[15] Dimitrios Makrakis, Abbas Yongacoglu, and Kamilo Feher, "Novel Receiver Structures for Systems Using Differential Detection," *IEEE Trans. on Veh. Tech.*, Vol. VT−36, May 1993, pp. 71−77.

[16] C. Liu and K. Feher, "Noncoherent Detection of $\pi/4$-QPSK of System in CCI-AWGN Combined Interference Environment," *Proceedings of the IEEE Vehicular Technology Conference*, San Francisco, 1989, pp. 83−94.

[17] W. W. Peterson, E. J. Welden, Jr., *Error Correcting Code*, 2nd Ed. Cambridge, MA: MIT Press, 1972.

[18] A. J. Viterbi, J. K. Omura, *Principle of Digital Communications and Coding*, McGraw-Hill, 1979.

[19] J. G. Proakis, *Digital Communications*, McGraw-Hill, Inc., 1989.

[20] M. Nakagami, "The m-distribution—A General Formula of Intensity Distribution of Rapid Fading," in W.G. Hoffman, Ed., *Statistical Methods in Radio Wave Propagation*, Oxford, England, Pergamon Press, 1960, pp. 3−36.

[21] C. W. Kim, *Analysis of BPSK System and Modulation Classification of PSK Signals over Nakagami Fading Channels*, M.Sc. thesis, Dep. Elec. Com. Eng., Hanyang Univ., Korea, Dec. 1995.

[22] R. W. Lucky, J. Salz and E. J. Weldon, Jr., *Principle of Data Communication*. McGraw-Hill, 1968.

[23] I. S. Gradshteyn and I.M.Ryzhik, *Table of Integral, Series and Products*, Academic Press, Inc. 1965.

[24] D. Makrakis, A. Yongacoglu, and K. Feher, "A Sequential Decoder for the Differential Detection of Trellis Coded PSK Signals," *Proc. ICC '88*, 1988, pp. 1433−1438.

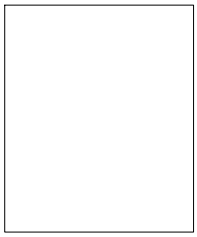

**Seog-Il Song** received the B.S. and M.S. degrees in electronics communication engineering from Hanyang University, Seoul, Korea in 1985 and 1987, respectively. Since 1987 he has been with Electronic and Telecommunications Research Institute. His research interests include mobile communication system, communication system performance evaluation, IMT-2000 and spread-spectrum systems.

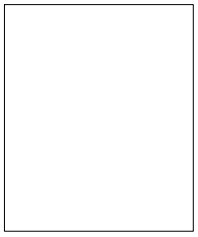

**Young-Yearl Han** received the B. S. degree from Seoul National University, Seoul, Korea in 1960, the M.S. and Ph. D. degrees from the University of Missouri-Rolla in 1976 and 1979, respectively, all in electrical engineering. Currently he is a professor at the Hanyang University, Seoul, Korea. His research interests are in the areas of statistical signal processing and communiaction theory as applied to analysis and evaluation of digital communication system, with a current emphasis on mobile and wireless communication. He is listed in Marquis "who's who in the world" in the 15th Edition. He is a senior member of IEEE and was a vice president of the Korea Institute of Communication Sciences from 1990 to 1995.